Organosoluble, Segmented Rigid-Rod Polyimide Films. 1. Structure Formation

Stephen Z. D. Cheng,* Fred E. Arnold, Jr., Anqiu Zhang, Steve L.-C. Hsu, and Frank W. Harris

Institute and Department of Polymer Science, College of Polymer Science and Polymer Engineering, The University of Akron, Akron, Ohio 44325-3909

Received March 11, 1991; Revised Manuscript Received June 21, 1991

ABSTRACT: A segmented rigid-rod polyimide has been synthesized from 3,3',4,4'-biphenyltetracarboxylic dianhydride (BPDA) and 2,2'-bis(trifluoromethyl)-4,4'-diaminobiphenyl (PFMB) in refluxing *m*-cresol. The polymer is soluble in hot phenolic solvents and can be solution cast into thin films. When the films are highly oriented, the polymer crystallizes in a monoclinic lattice with a = 15.40 Å, b = 9.918 Å, c = 20.21 Å, and γ = 56.2°. When unoriented films are annealed at 425 and 450 °C, an in-plane orientation process of the crystals and chain molecules takes place, so that the crystals' c axes end up parallel to the films' surfaces. This is followed by further structure development where the apparent crystal size increases with annealing time and temperature. It is postulated that the long-range molecular motion required for orientation is facilitated by residual solvent in the film. Avrami exponents for the structure development support a molecular-motion-controlled process.

Introduction

Aromatic polyimides exhibit excellent electrical and mechanical properties, along with high thermal and thermooxidative stability. The polymers also display chemical and solvent resistance, good adhesive properties, and light and dimensional stability. This unique combination of properties has led to wide industrial high-temperature applications in films, fibers, coatings, adhesives, and matrix materials in polymer composites. However, aromatic polyimides are difficult to process because they are insoluble in conventional solvents and do not flow below their decomposition temperatures. In fact, they are usually processed in the form of their poly(amic acid) precursors.

Among the many industrial polyimide products, polyimide films are especially important. They are widely used in applications such as interlayer dielectrics in multilevel very large-scale integrated circuits. Perhaps the most used film is that prepared from poly(4,4'-oxydiphenylenepyromellitimide) (PMDA-ODA), which is commercially produced by Du Pont under the tradename of Kapton.[1,2]

PMDA-ODA is obtained from the polycondensation of pyromellitic dianhydride (PMDA) with 4,4'-oxydianiline (ODA). The reaction initially produces poly(amic acid), which is solution cast into film to form PMDA-ODA. The film is then heated so that the poly(amic acid) is imidized (cyclodehydrated). This "curing" process eliminates any solvents as well as the water, condensation byproduct. The heating process also results in changes in morphology and properties.

An earlier study of PMDA-ODA fibers, which utilized wide-angle X-ray diffraction (WAXD), showed that the polymer's unit cell is orthorhombic with lattice parameters of a = 6.31 Å, b = 3.97 Å, and c = 32 Å.[3,4] The chain was also determined to be in a 2_1 helical conformation along the c axis. Small-angle X-ray scattering (SAXS) measurements showed a long spacing of 230 Å along the fiber axis.[5,6] However, the morphologies of PMDA-ODA films have not been readily deduced. Morphologies ranging from structureless glass[7,8] to semicrystalline[9,10] have been reported. A significant orientation of the molecules parallel to the surface of a thin film (in-plane orientation) has also been observed.[11,12] Isoda et al. demonstrated that the curing temperature was important in the development of this morphology.[13] On the basis of WAXD and SAXS experiments, they proposed that the average orientation of the segments within the aggregates was perpendicular to the direction of periodicity, which is an unusual morphology that has not been previously observed in polymer crystals. Russell later reported SAXS and WAXD data that did not support this morphology.[14] On the other hand, Takahashi, Yoon, and Parrish presented WAXD data on a poly(amic acid) film containing ~30% solvent that showed that the chains were aligned parallel to the film surface. The highly extended chain segments (~14 Å) displayed correlated (smecticlike) lateral packing. This order could be improved by imidization, solvent removal, and an increase of the curing temperature. Nevertheless, no long-range crystalline order was found.[15] Fluorescence spectroscopy has been used to monitor the degree of "cure" and the effect of curing history on the morphological changes in this polyimide.[16]

Recently, a family of organosoluble, rigid-rod, and segmented rigid-rod aromatic polyimides was synthesized in our laboratory.[17] These polyimides were prepared in refluxing *m*-cresol in a one-step process where the intermediate poly(amic acids) were not isolated. Upon cooling to near 120 °C, the polyimide solutions set to gellike structures. The gel/sol transitions of these solutions depended upon the polymer's concentration, the polymer's molecular weight, and the chain's rigidity. Upon standing, lyotropic liquid-crystalline structures formed in the gels.[18] Some of these polyimides exhibited excellent fiber-forming tendencies, and high-performance, oriented fibers were prepared. Through the study of these fibers, the polyimides' crystal unit cell dimensions were determined.[19]

In this series of papers, we will report the results of our studies of the films made from one of these segmented rigid-rod polyimides. This polyimide can be crystallized both in solution[20] and in the solid state.[19] In this paper, the structure formation of the crystal in the film will be described. This will include a description of the in-plane chain orientation in the crystal, the crystal formation kinetics, the crystal sizes, and the film dimensional changes that take place during annealing.

Experimental Section

Materials. The polyimide was synthesized from 3,3',4,4'-biphenyltetracarboxylic dianhydride (BPDA) and 2,2'-bis(triflu-

0024-9297/91/2224-5856$02.50/0

oromethyl)-4,4′-diaminobiphenyl (PFMB) in refluxing *m*-cresol. The chemical structure is

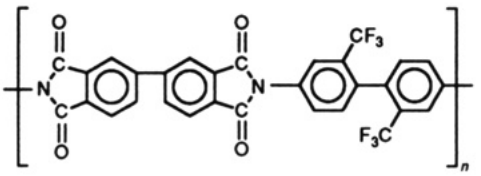

with a repeating unit of 578.5 g/mol. The detailed experimental procedure has been reported elsewhere.[17] Thus, both the dianhydride and diamine were dissolved in *m*-cresol to a total monomer concentration of 10% (w/w). The resulting solution was heated at reflux for 4 h. Although the polymer remained completely in solution during the polymerization, the polymerization mixture set to a gellike structure when it was cooled below about 120 °C. Upon standing, lyotropic liquid-crystalline structures developed in the gel. A detailed description of the gel/sol and liquid-crystal transitions have been reported elsewhere.[18] The intrinsic viscosity of the polyimide BPDA–PFMB in *m*-cresol at 30 °C was 4.9 dL/g.

Film Preparation. BPDA–PFMB films were prepared by spreading a 2% (w/w) *m*-cresol solution on a glass plate with a doctor's knife, followed by drying at 150 °C for 5 h under reduced pressure in a vacuum oven (VWR-1410D). In this manner, films were prepared with thickness ranging from 10 to 15 μm. Precise control of the solution's concentration and the thickness of the casting dope on the glass plate was necessary to control the final thickness of the film.

In order to study the crystal structure of the polyimide, the film was oriented under tension at 400 °C. The film was elongated up to 700% and then annealed at 420 °C for 15 min under tension to fully develop the crystallinity. On the other hand, unoriented films were used to investigate the structure formation.

Equipment and Experiments. Wide-angle X-ray diffraction (WAXD) experiments were conducted by using a Rigaku X-ray generator with a 12-kW rotating anode. The point-focused beam was monochromatized by a graphite crystal sensitive to Cu Kα radiation. Both reflection and transmission geometrical modes were carried out on a Rigaku diffractometer. The 2θ angle range for these two modes is between 5° and 50°. Special care was taken to avoid false scattering at small diffraction angles. A typical experimental run took about 4 h, with the generator operating at 8 kW with a scanning speed of 0.2°/min. Background runs were frequently recorded in order to obtain precise background subtractions.

A single, flat film was isothermally annealed in a high-temperature oven for different annealing times under a dry-nitrogen atmosphere. Annealing temperatures of 425 and 450 °C were used (the decomposition temperature is lower than the melting temperature). The annealing time was usually short, ranging from a few seconds to 0.5 h. After annealing, the film thickness and weight loss were measured. The film was then mounted on an aluminum sample holder for WAXD measurements. The typical film size was 1.5 × 1.5 cm².

The samples' apparent crystallinities (w^*) were calculated by substracting the WAXD patterns of unannealed films from that of annealed ones in both modes after correcting for residual solvent content. Apparent crystal sizes along certain crystallographic planes were calculated by using the Scherrer equation

$$L = K\lambda/[(B^2 - b^2)\cos\theta]^{1/2}$$

where B and b are the half-width of the diffraction peak and the broadening factor ($b = 0.5$, which was determined by equipment calibration), respectively, and K is a geometry-dependent constant, which is assumed to be 0.9.

Crystal unit cell parameters were determined with a plate vacuum camera, which was used to take WAXD photographs on uniaxially oriented films. The d spacings were calibrated with silicon powder with a 325-mesh size.

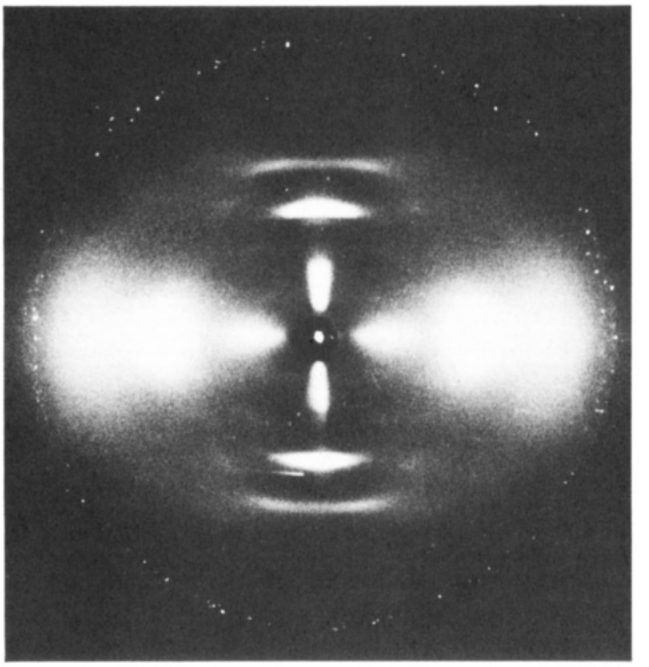

Figure 1. WAXD photodiagram of a highly oriented BPDA–PFMB film.

Table I
Experimental and Calculated Crystallographic Parameters of the Monoclinic Crystal Unit Cell for BPDA–PFMB Films[a]

	2θ, deg		d spacing		
(hkl)	exptl	calcd	exptl	calcd	intensity[b]
(100)	6.894	6.906	12.82	12.80	w
(200)	13.79	13.84	6.422	6.399	m
(310)	17.13	17.29	5.177	5.129	s
(420)	24.02	23.90	3.704	3.723	m
(001)	4.370	4.372	20.22	20.21	s
(101)	8.184	8.177	10.79	10.81	w
(002)	8.738	8.750	10.12	10.10	m
(102)	11.59	11.16	7.634	7.931	w
(003)	13.11	13.14	6.753	6.737	vs
(213)	17.75	17.76	4.997	4.985	m
(004)	17.60	17.55	5.038	5.053	m
(104)	18.90	18.88	4.690	4.700	m
(014)	20.63	20.62	4.300	4.307	w
(005)	22.12	21.99	4.019	4.042	w
(006)	26.58	26.46	3.353	3.368	w
(007)	31.80	30.97	2.814	2.887	w

[a] The calculated data for 2θ and d spacing is based on a monoclinic crystal unit cell of $a = 15.40$ Å, $b = 9.918$ Å, $c = 20.21$ Å, and $\gamma = 56.2°$. [b] Intensity was semiquantitatively measured through a microdensitometer and classified by very strong (vs), strong (s), medium (m), and weak (w).

Results

Determination of the Crystal Unit Cell. Figure 1 shows a WAXD photograph (fiber pattern) for the uniaxially oriented films. Along the equator, there are four diffraction spots that can be identified. Along the meridian, periodic diffraction spots can be clearly observed for up to seven layers. On the quadrants, one spot can be identified along the first, second, and third layers, and two spots can be identified along the fourth layer. Overall, 16 diffraction spots can be observed. A detailed listing of the experimental 2θ angles, d spacings, and corresponding intensities of the diffraction spots are given in Table I.

To determine the size and shape of the crystal unit cell for our oriented film diagrams, we ordinarily begin by trying to find an $hk0$ reciprocal lattice net, namely, a

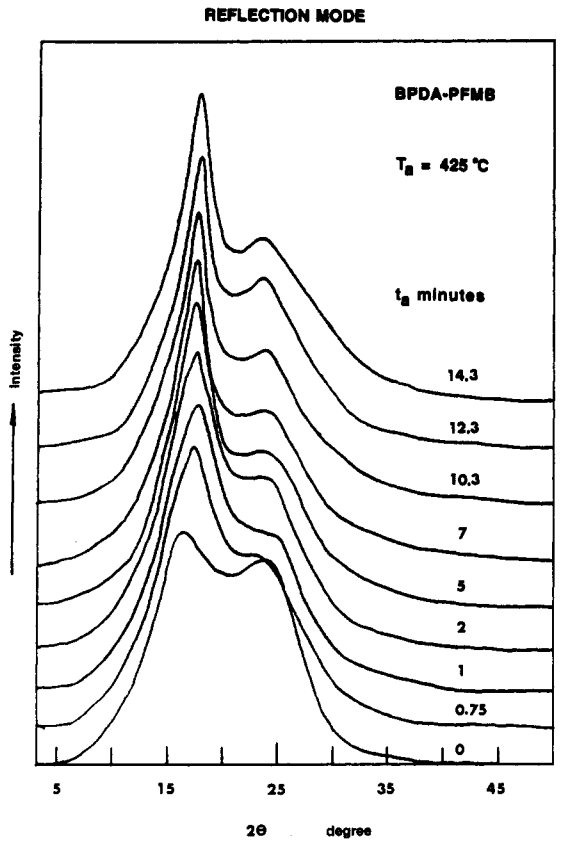

Figure 2. Set of WAXD patterns obtained through the reflection mode for BPDA–PFMB films annealed at 425 °C.

parallelogram with edges a^* by b^* that account for the values determined from the equatorial diffractions. The smallest distance between the center of the X-ray incident beam and the diffraction spot corresponds to a low index. From Figure 1, one finds that this reciprocal lattice net can be formed, and all other diffraction spots can be fitted into this net. The l index of each diffraction can also be determined by the layer line on which the diffraction lies, and the c crystallographic axis is readily determined from the layer line spacing. After least-square refinements, we found that the crystal unit cell of the oriented BPDA–PFMB film is monoclinic with a = 15.40 (±0.04) Å, b = 9.918 (±0.04) Å, c = 20.21 (±0.04) Å, and γ = 56.2° (±0.2°). This leads to a crystallographic volume of 2566 Å^3. In each unit cell four repeating units are contained. The calculated crystallographic density is thus 1.50 g/cm^3. The calculated 2θ and d spacings are also included in Table I.

WAXD Patterns in Reflection Mode. Figure 2 gives a set of WAXD patterns for BPDA–PFMB films annealed at 425 °C, as an example. The annealing time ranges from 0 (unannealed) to 15 min. It is clear that unannealed films show some structure, indicating that they are not fully amorphous. However, it is evident that with increasing annealing time, an additional structure develops that increases the intensity of the crystallographic planes. In particular, the most dominant diffraction peak is at 2θ = 17.13°. This corresponds to the (310) crystallographic plane. Figure 3 illustrates the Avrami treatment for this development at two annealing temperatures (425 and 450 °C) by plotting the relationship between log [−ln (1 − w^*)] and log t_a, where w^* is the apparent crystallinity obtained from Figure 2. It is clear that the development of crystallinity at the higher temperature (T_a = 450 °C) is faster. Furthermore, two steps of crystalline development can be identified at both temperatures. The initial step shows an Avrami exponent of n that is close to 1.0, while

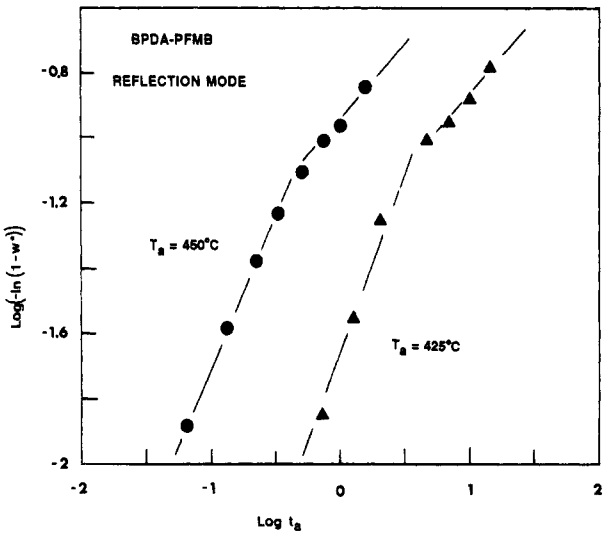

Figure 3. Avrami plots between log [−ln (1 − w^*)] and log t_a for the films annealed at 425 and 450 °C. The apparent crystallinity was measured through the reflection mode.

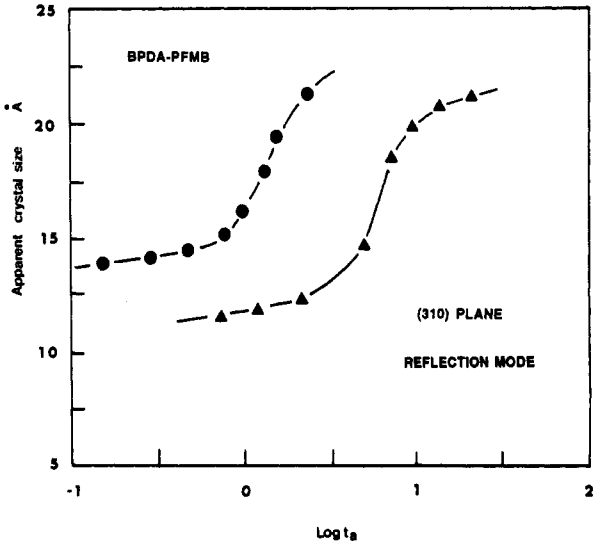

Figure 4. Relationship of apparent crystal size along the (310) plane with annealing time at both temperatures.

in the second step, n is in the vicinity of 0.5.

As shown in Figure 2, the diffraction peak of the (310) crystallographic plane becomes sharper, and the half-width of the peak decreases upon extended annealing. In Figure 4, which is based on the Scherrer equation, the relationship between the apparent crystal size along the (310) plane is plotted with respect to the logarithmic annealing time. It is not surprising to find that the apparent crystal size increases with both annealing time and temperature.

WAXD Patterns in Transmission Mode. Figures 5–7 show parallel results for the BPDA–PFMB films annealed at 425 and 450 °C obtained with a WAXD transmission mode. It is interesting that the dominant diffraction peak is at 2θ = 13.11°, which corresponds to the (003) crystallographic plane (Figure 5). A shoulder at 2θ = 17.60° is due to the (004) plane. Most importantly, one cannot observe the (310) diffraction peak (at 2θ = 17.13°) in this mode. With increasing annealing time, the development of the apparent crystallinity is obvious. This can also be treated with the Avrami equation, as shown in Figure 6. However, in this case, the Avrami exponent n is close to 0.5 for the initial crystallization step and near 0.1 for the second step at both T_a = 425 and 450 °C. Figure 7 shows the development of the apparent crystal size along

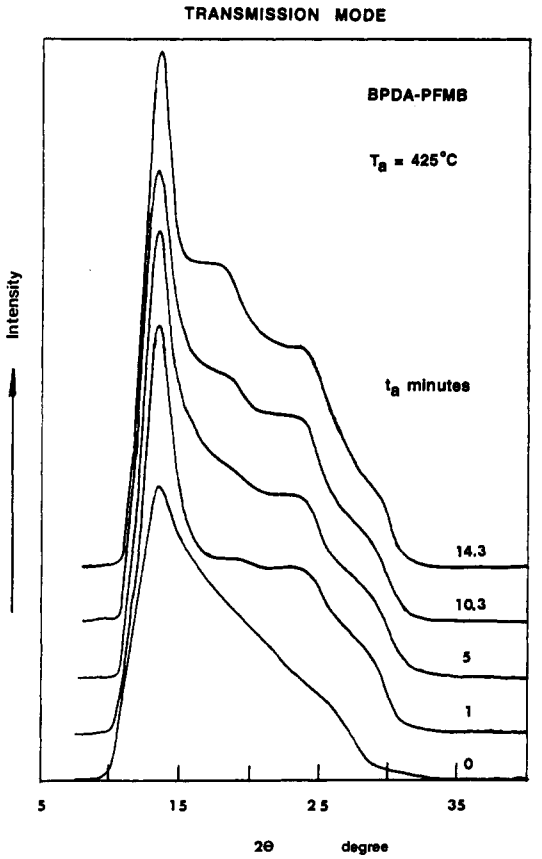

Figure 5. Set of WAXD patterns obtained through the transmission mode for the films annealed at 425 °C.

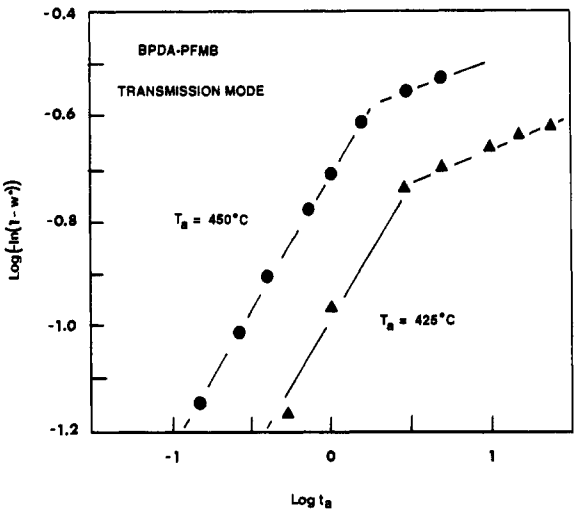

Figure 6. Avrami plots similar to Figure 3 but with the apparent crystallinity measured through the transmission mode.

the (003) crystallographic plane during annealing. Similar to Figure 4, there is an increase in size with temperature and time.

Size and Weight Changes during Annealing. Figure 8 reflects the decreases in reduced film thickness (l/l_0) that occur with increasing annealing time at T_a = 425 and 450 °C in a dry-nitrogen atmosphere. The major portion of these decreases occurs early in the annealing period. After 8.5 min at 425 °C and after 7.5 min at 450 °C, the thicknesses remain constant throughout the remainder of the annealing period. Thus, the films retain 78% of their initial thickness. The reduced weight (w/w_0) also decreases with increasing annealing time. The overall weight loss is about 15%, which occurs within 2.0 min at 425 °C and

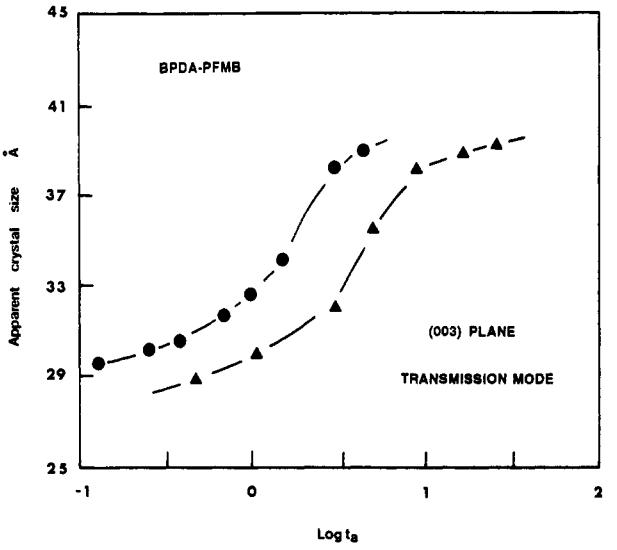

Figure 7. Apparent crystal size changes along the (003) plane with annealing time at both temperatures.

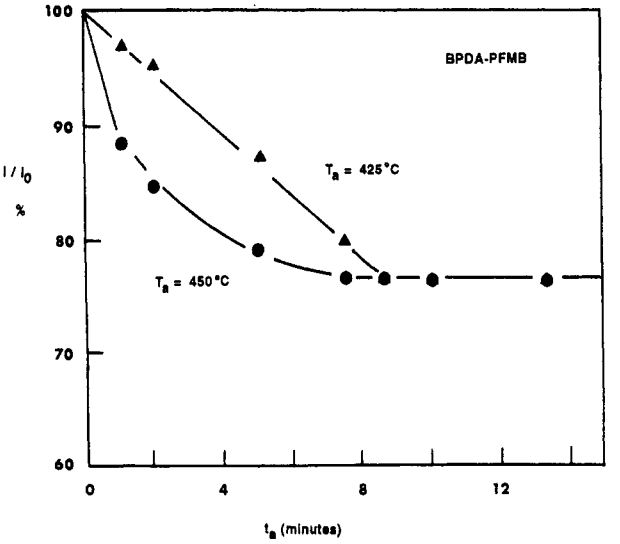

Figure 8. Reduced film thickness changes with annealing time at both temperatures.

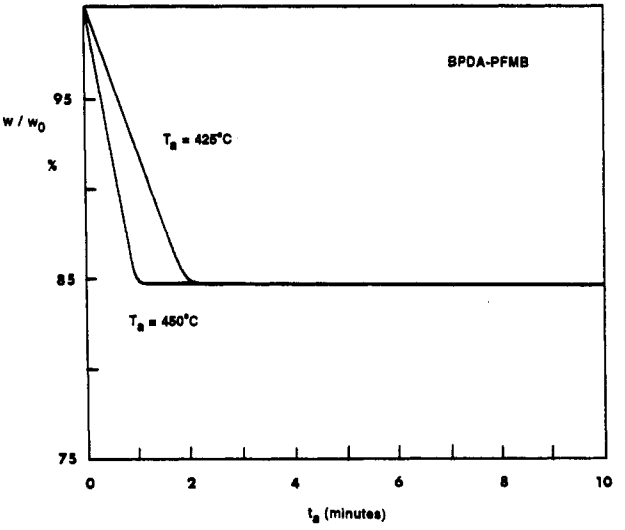

Figure 9. Reduced film weight-loss changes with annealing time at both temperatures.

within 1.0 min at 450 °C. Further increases in annealing time do not lead to additional weight losses. During the first few minutes of the annealing, clear evidence of the

evaporation of residual *m*-cresol was obtained by using thermogravimetry measurements coupled with mass spectroscopy.[21]

Discussion

This is the first part of our study of the films of the segmented rigid-rod polyimide. Our focusing points were the crystal structure formation and chain orientation. In future papers, the film's dimensional stability (TEC), crystal morphology, and dielectric and optical properties will be discussed.

The crystal unit cell size and shape obtained from highly oriented BPDA–PFMB films (Figure 1 and Table I) are very close to those observed in the polymer's fibers where a = 15.40 Å, b = 9.90 Å, c = 20.25 Å, and γ = 56°.[19] Both materials crystallized in a monoclinic lattice. This should not be surprising since the chemical structure of the polymer is the same in both. However, it is evident that the WAXD pattern shown in Figure 1 has more diffraction spots than that obtained on the BPDA–PFMB fibers. This is perhaps due to the fact that the pattern obtained in Figure 1 was taken by using a single thin film, while the photograph of the fibers was obtained from a bundle of fibers. In particular, the c axis in the film's unit cell (20.21 Å) shows the most deviation from the corresponding dimension in the fiber's unit cell (20.25 Å). However, it is well-known that the length of the c axis is draw-ratio dependent.[19] In fact, when the fibers were only drawn about seven times, it displayed a c axis of 20.21 Å[19] (please note that the film was drawn 700% (or seven times) before the WAXD measurements). The slight differences in the b axes may also be due to different draw ratios and/or annealing conditions.

The annealing process at the two different temperatures led to changes in both molecular orientation and structure. It is evident that the chain molecules in the crystals of as-cast films are not fully in-plane oriented. This is evident from the WAXD patterns of the films in both the reflection and transmission modes (Figures 2 and 5). The broad diffraction peak with a relatively high intensity at 2θ = 13.11° [corresponding to the (003) plane, see Table I] in the pattern obtained with the transmission mode indicates that some small crystals exist, with their c axis more or less parallel to the film surface. However, the diffraction peak observed with the reflection mode around 2θ = 16.0° is most likely due to an overlap of several crystallographic planes such as the (310) and (003) planes [please note that the diffraction peak of the (310) plane is at 2θ = 17.13° (see Table I)]. As a consequence, one may expect that the c axis of these crystals is somewhat randomly distributed between a parallel orientation and a perpendicular orientation relative to the film surface, in which the parallel orientation is in the majority.

As soon as the films are annealed, even for a very short period of time, the WAXD patterns in both modes change as shown in Figures 2 and 5. The reflection pattern contains a (310) diffraction peak at 2θ = 17.13°, which results from a shift in the overlapped diffraction peak at around 2θ = 16.0°. On the other hand, the diffraction peak of the (003) plane observed with the transmission mode is enhanced. It is significant that the WAXD pattern obtained with the reflection mode after annealing is similar to the WAXD fiber pattern (Figure 1) scanned along the equatorial direction and that the transmission pattern is almost identical with the WAXD fiber pattern scanned along the meridian direction, as shown in Figures 10 and 11. It is obvious that in the WAXD fiber pattern the diffraction spots along the equatorial direction are representative of the (hk0) crystallographic planes, and those along the meridian direction are due to the (001) crystallographic planes. One can, thus, conclude that the chain molecular orientation in the crystal is in-plane after

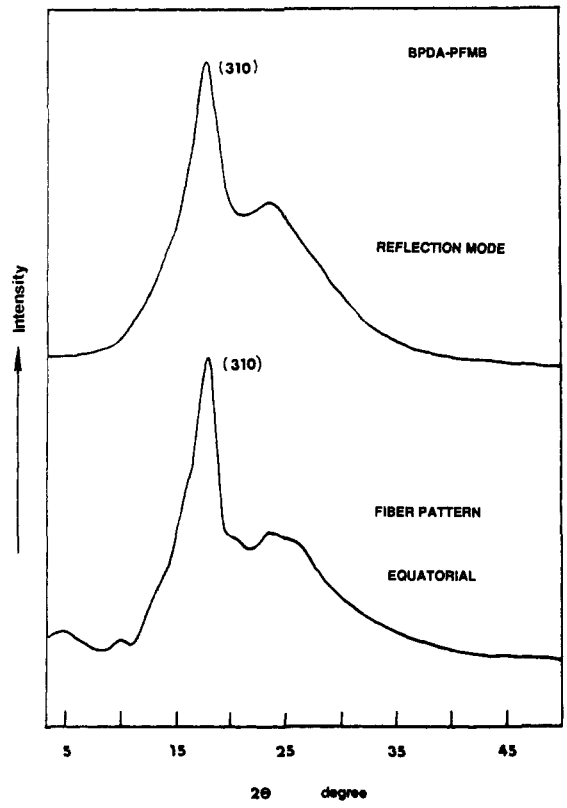

Figure 10. Comparison of WAXD patterns obtained through the reflection mode of BPDA–PFMB films and scanned along the equatorial direction of Figure 1.

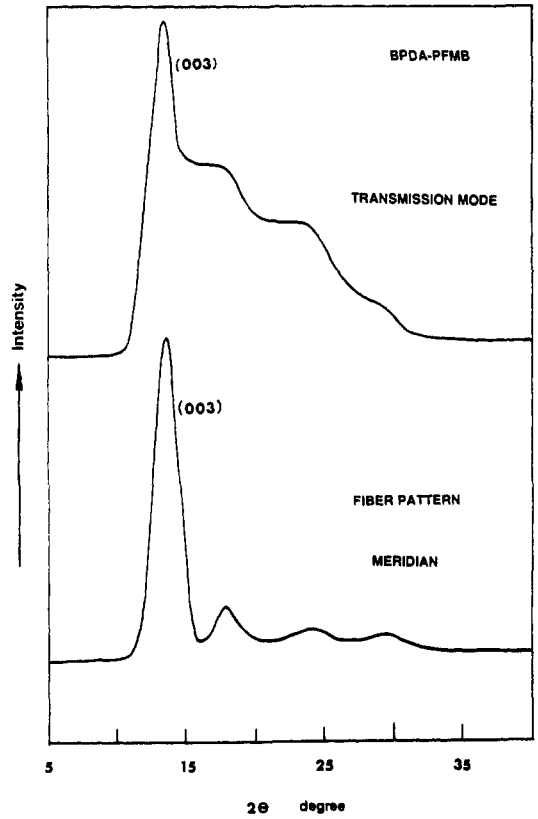

Figure 11. Comparison of WAXD patterns obtained through the transmission mode of the films and scanned along the meridian direction of Figure 1.

annealing. That is, the chain direction is parallel to the film surface. The only difference between the film and the fiber is that the c axis of the crystals is randomly distributed in the film, while that in the fiber is oriented along the draw direction.

The origin of the assumed anisotropy in the film may lie in the confinement of the long, rigid chains in a limited space. On the basis of intrinsic viscosity data, the length of the BPDA–PFMB chain has been estimated at about 2000 Å or 0.2 μm. This is only about 1 order of magnitude smaller than the film thickness. Although it is not completely clear how this large-scale molecular motion can take place, it is apparent that at the annealing temperatures the in-plane orientation of the segmented rigid-rod chain is thermodynamically more stable than other arrangements. On the basis of the fact that no evidence for the c-axis orientation perpendicular to the film surface could be found and the fact that the chains are stiff, it is also likely that the in-plane crystal orientation reflects the orientation of the entire chain. Since the chain length is about 2 orders of magnitude longer than the crystal size, it is postulated that single chains run through more than one crystalline region. We will test this speculation through an extensive study of crystal morphology, computer modeling, and calculation. It is interesting to compare the chain orientations in the BPDA–PFMB films, which are evidently similar to those in films of PMDA–ODA,[12-15] with those in films prepared from more flexible polymers. The c-axis crystal orientation in solution-cast films of flexible linear polymers, such as polyethylene and other polyolefins, is usually perpendicular to the surface of the films.[22] In this case, however, the chain flexibility allows the molecules to undergo extensive chain folding during the formation of lamellae. In order to minimize the surface free energy, the lamellae stack parallel to the film surface, which results in a perpendicular c-axis orientation.

In order to learn more about the process by which the stiff chains assume their in-plane orientation, changes in reduced film thickness and weight were monitored during thermal annealing (Figures 8 and 9). The weight-loss measurements revealed that, during the first few minutes of annealing, the films lost approximately 15% of their total weight. Since the polymer has been shown to be stable at the annealing temperatures,[21] the weight loss can be attributed to the loss of residual m-cresol. The presence of this solvent undoubtedly facilitates the large-scale molecular motion necessary for the chains to assume their in-plane orientation. In fact, the degree of orientation is essentially unchanged after the solvent is lost. However, the film does continue to thin; i.e., the point at which the weight loss reaches a constant value is almost 7 min earlier than the point where the film thickness becomes essentially fixed. The decrease in the thickness after the loss of solvent can be attributed to the increase in density associated with the continuous structure development.

In order to learn more about the kinetics of crystal formation, the crystallization data was analyzed in terms of the Avrami expression.[23] Thus, in the initial annealing stages, the crystals along the ($hk0$) planes, whose development was followed using a reflection mode, have an Avrami exponent of approximately 1.0 (Figure 3), while those along the (001) planes, whose development was followed by using a transmission mode, have an Avrami exponent of approximately 0.5 (Figure 6). For a two-dimensional system with oriented rigid macromolecules growing parallel to the surface, the Avrami exponent is 2.0 in the case of athermal nucleation. Similarly, athermal nucleated one-dimensional growth leads to an Avrami exponent of 1.0.[24] However, if long-range molecular motion is involved in the rate-determining step in structure formation, the rate of formation is $t^{-1/2}$ dependent.[25] As a result, the Avrami exponent for two-dimensional group is 1.0 and 0.5 for one-dimensional growth. These values correspond well to our experimental observations. Nevertheless, it should be pointed out that the presence of solvent in the initial stage of the structure development may obscure this Avrami application, although a correction of the solvent content has been made in our data treatment.

Of particular interest are the points in Figures 4 and 7 where the plots undergo significant changes in slope. The points are close to those where the apparent crystal sizes start increasing. This indicates that a secondary crystallization process represented by lower Avrami exponents is responsible for the further increase in crystallinity through crystallization of disordered molecules and perfection of the crystal through a decrease in defects, and therefore an increase in crystal size.

Conclusion

The crystal unit cell of highly oriented BPDA–PFMB films is monoclinic with a = 15.40 Å, b = 9.918 Å, c = 20.21 Å, and γ = 56.2°. The structure formation in unoriented BPDA–PFMB films during annealing can be monitored by using reflection and transmission WAXD modes. Microscopically, the crystallographic c axis undergoes an orientation process, which results in its being parallel to the film surface during the initial stages of annealing. This also results in an in-plane chain orientation in the films. The apparent crystal size increases with time during the annealing process. Macroscopically, the structure formation can be described by using the Avrami expression. The Avrami exponents indicate that the crystal growth along the ($hk0$) and (001) crystallographic planes is controlled by long-range molecular motion.

Acknowledgment. This work was supported by the Material Research Division of the National Science Foundation (DMR-8920147) through the Science and Technology Center of the Advanced Liquid Crystals for Optical Materials (ALCOM) at Kent State University, The University of Akron, and Case Western Reserve University. The synthesis of this segmented rigid-rod polyimide was supported by a NASA–Langley Research Center Grant (NAG-1-448).

References and Notes

(1) Lee, H.; Stoffey, D.; Neville, K. *New Linear Polymers*; McGraw-Hill: New York, 1967; pp 183 and 224.
(2) Sroog, C. E. *J. Polym. Sci., Macromol. Rev.* **1976**, *11*, 161.
(3) Tuichiev, Sh.; Korzhavin, L. N.; Prokhov, O. Ye; Ginsburg, B. M.; Frenkel, S. Ya. *Vysokomol. Soedin., Ser. A* **1971**, *13*, 1463.
(4) Kazaryan, L. G.; Tsvankin, D. Ya.; Ginsburg, B. M.; Tuichiev, Sh.; Korhavin, L. N.; Frenkel, S. Ya. *Vysokomol. Soedin., Ser. A* **1972**, *14*, 1199.
(5) Slutsker, L. I.; Utevskii, L. Ye.; Chereiskii, Z. Yu.; Perepelkin, K. E. *J. Polym. Sci., Polym. Symp.* **1977**, *58*, 399.
(6) Slutsker, L. I.; Utevskii, L. Ye.; Chereiskii, Z. Yu.; Stark, I. M.; Mińkova, N. D. *Vysokomol. Soedin., Ser. A* **1973**, *15*, 2373.
(7) Rudakov, A. P.; Bessonov, M. I.; Koton, M. M.; Pokrovskii, Ye. I.; Fedorova, Ye. F. *Dokl. Akad. Nauk SSSR* **1965**, *161*, 617.
(8) DeIasi, R.; Russel, J. *J. Appl. Polym. Sci.* **1971**, *15*, 2965.
(9) Ushakov, G. P.; Grushko, Yu. A.; Lazurkin, Yu. S.; Kazakov, V. S. *Vysokomol. Soedin.* **1960**, *2*, 1512.
(10) Lúre, Ye. G.; Kazaryan, L. G.; Uchastkina, E. L.; Kovriza, V. V.; Vlasova, K. N.; Dobrokhotova, M. L.; Yemel, Y. *Vysokomol. Soedin., Ser. A* **1971**, *13*, 603.
(11) Ikeda, R. M. *J. Polym. Sci., Polym. Lett. Ed.* **1966**, *4*, 353.
(12) Russell, T. P.; Gugger, H.; Swalen, J. D. *J. Polym. Sci., Polym. Phys. Ed.* **1983**, *21*, 1745.

(13) Isoda, S.; Shimada, H.; Kochi, M.; Kambe, H. *J. Polym. Sci., Polym. Phys. Ed.* **1981**, *19*, 1293.
(14) Russell, T. P. *J. Polym. Sci., Polym. Phys. Ed.* **1984**, *22*, 1105.
(15) Takahashi, N.; Yoon, D. Y.; Parrish, W. *Macromolecules* **1984**, *17*, 2583.
(16) Wachsman, E. D.; Frank, C. W. *Polymer* **1988**, *29*, 1191.
(17) Harris, F. W.; Hsu, S. L.-C. *High Perform. Polym.* **1989**, *1*, 1.
(18) Cheng, S. Z. D.; Lee, S.-K.; Barley, J. S.; Hsu, S. L.-C.; Harris, F. W. *Macromolecules* **1991**, *24*, 1883.
(19) Cheng, S. Z. D.; Wu, Z.-Q.; Eashoo, M.; Hsu, S. L.-C.; Harris, F. W. *Polymer* **1991**, *32*, 1803.
(20) Heberer-Smith, E. M. S. Thesis, Department of Polymer Science, The University of Akron, Akron, OH 44325-3909.
(21) Arnold, F. E., Jr.; Cheng, S. Z. D.; Hsu, S. L.-C.; Harris, F. W., in preparation.
(22) Kyu, T.; Fujita, K.; Cho, M.-H.; Kikutani, T.; Lin, J. S. *Macromolecules* **1989**, *22*, 2238.
(23) Avrami, M. *J. Chem. Phys.* **1939**, *7*, 1103; **1940**, *8*, 212; **1941**, *9*, 177.
(24) Wunderlich, B. *Macromolecular Physics, Crystal Nucleation, Growth, Annealing*; Academic Press: New York, 1976; Vol. 2.
(25) Cheng, S. Z. D. *Macromolecules* **1988**, *21*, 2475; **1988**, *21*, 3327.

Registry No. (BPDA)(PFMB) (copolymer), 129219-16-5; (BPDA)(PFMB) (SRU), 129219-45-0.